IL NUOVO CIMENTO Vol. 36 C, N. 2 Marzo-Aprile 2013
DOI 10.1393/ncc/i2013-11510-x

Colloquia: Nanoforum 2012

Innovative nanomaterials for fuel cells fed with biogas

F. Zaza([1])([2])(*), M. Pasquali([2]), E. Simonetti([1]),
C. Paoletti([1]) and A. Dell'Era([3])

([1]) *ENEA-Casaccia R.C. - Via Anguillarese 301, 00123 S. Maria di Galeria (RM), Italy*
([2]) *University of Rome Sapienza - Via del Castro Laurenziano 7, 00161 Rome, Italy*
([3]) *CIRPS - Via Eudossiana 18, 00184, Rome, Italy*

ricevuto il 17 Marzo 2013

Summary. — Challenges on sustainability promote research policy focused on renewable-energy technology development in order to enhance global energy security, local energy independence, environmental protection and economic growth. Biomass resources offer renewable energies that can play a key role in the current global strategies for reducing greenhouse gas emissions by partially replacing fossil fuels. The conversion of biomass chemical energy into electrical energy and cogenerated heat can be obtained by fuel cells. In particular, molten carbonate fuel cell (MCFC) is the most suitable device for bioenergy production because it can be fed directly with biogas, whose primary constituents all improve the performance of the cell. However hydrogen sulfide, which is the main biogas impurity, poisons the traditional nickel based anode, affecting the power and the endurance of the cell. In order to overcome this problem, an innovative anode material that resists against the sulfide corrosions has been developed. This material, made of a nanostructured and porous nickel support covered with a thin layer of ceria, exhibits high sulfur tolerance and recovering capability.

PACS 88.20.-j – Biomass energy.
PACS 68.55.-a – Thin film structure and morphology.
PACS 88.30.M- – Fuel cell component materials.
PACS 88.30.pm – Molten carbonate fuel cells.

1. – Introduction

The need for global energy security, local energy independence, environmental protection and socio-economic growth drives toward technology promoting alternative energy sources, such as nuclear and renewable sources. The latter is the most interesting one

(*) E-mail: fabio.zaza@enea.it, fabio.zaza@uniroma1.it

Fig. 1. – Integrated system regarding the bioenergy production from fuel cell fed with biogas.

due to the difficulties on nuclear waste management of the former [1]. The production of bioenergy by fuel cells address this challenge combining the advantage of both biomass [2, 3] and fuel cell device [4-9]: biomass is an available, renewable, sustainable and carbon based energy source; fuel cells are sustainable and efficient energy conversion devices. An integrated system, fig. 1, where fuel cell device is fed with biogas produced from anaerobic digestion of organic waste, promotes mutual synergistic connections between biomass and fuel cell [10]. The main drawback of biomass is that it has low-energy contents because it consists of partially oxidized organic matter. The utilization of fuel cell devices minimizes that problem because almost all chemical energy is converted to electricity and heat. In the same time, the main disadvantage of fuel cell device is that it has to be fed with hydrogen, whose production has adverse environment effects because it currently occurs by fossil fuels reforming processes. The utilization of biomass as hydrogen supplier minimizes that difficulty because the biohydrogen production is both energetically and economically sustainable. The most interesting biofuel for the integrated system is the waste-derived biogas, whose utilization gives several advantages. In general, biogas, whose components include methane and carbon dioxide mainly, has a significant Higher Heating Value, typically around $22.9\,\mathrm{MJ/m^3}$. In particular, waste-derived biogas promotes the waste managing in landfill sites by its reutilization. Also, it promotes the mitigation of greenhouse gas by replacing the uncontrolled methane emissions produced during the natural biomass biodegradations in landfill sites with the controlled methane emissions into anaerobic digesters. Finally, the reforming of light hydrocarbons, right as methane, is kinetically favored. The most interesting fuel cells for the integrated system are high-temperature fuel cells, including Solid Oxide Fuel Cells and Molten Carbonate Fuel Cells. Indeed, they are able to perform internal reforming of low molecular weight hydrocarbons because the heat required to sustain the endothermic global reforming reaction can be provided by the cogenerated heat from electrochemical reactions. In addition, the carbon monoxide is not a poison, but it is a fuel by the direct electrode reaction and also a hydrogen supplier by the water gas shift reaction. Among the high-temperature fuel cells, Molten Carbonate Fuel Cells are particularly suitable because both the main biogas components are useful reactants: methane is a fuel by the direct electrode reaction and also a hydrogen supplier by the reforming reaction; carbon dioxide, even though it inhibits the overall electrochemical reaction in agreement with the Le Chatelier's principle, promotes cell performance because it inhibits the electrolyte

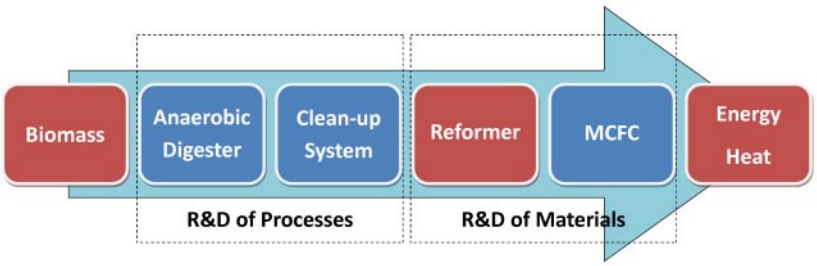

Fig. 2. – Block diagram for the integrated system where the unit processes are schematically represented.

loss. The main problem in MCFC fed with biogas is the hydrogen sulfide poisoning that affect the cell performance, including the power output and the durability [11-15]. Considering the unit processes in the integrated system, fig. 2, the sulfur poisoning issue is addressed by process developing for both the anaerobic digestion step in order to produce biogas with low amount of hydrogen sulfide and the clean-up step in order to remove high amount of hydrogen sulfide. In addition, the sulfur poisoning issue is addressed by material developing for both the reforming and energy conversion steps in order to have catalysts with improved sulfur resistance. In order to identify materials having high sulfur resistance, it is useful to understand the poisoning mechanism. In general, hydrogen sulfide affects cell performance because it reacts with both the anode and the electrolyte: carbonates react with hydrogen sulfide and produce sulfide and sulfate ions; nickel reacts with hydrogen sulfide with different reaction pathways and mechanisms, such as bulk chemical reactions (1), chemisorptions (2), physical adsorption (3) and electrochemical reactions (4):

$$x\mathrm{Ni} + y\mathrm{H_2S} \rightarrow \mathrm{Ni}_x\mathrm{S}_y + y\mathrm{H_2}, \tag{1}$$

$$\mathrm{Ni} + \mathrm{H_2S} \rightarrow \mathrm{NiS} + \mathrm{H_2}, \tag{2}$$

$$\mathrm{Ni} + \mathrm{H_2S} \rightarrow \mathrm{Ni} - \mathrm{H_2S}, \tag{3}$$

$$x\mathrm{Ni} + y\mathrm{H_2S} + y\mathrm{CO_3^{=}} \rightarrow \mathrm{Ni}_x\mathrm{S}_y + y\mathrm{CO_2} + y\mathrm{H_2O} + 2xe^{-}. \tag{4}$$

Previous experimental and computational analyses were performed to study poisoning mechanisms. Results showed that the cell performances are affected by anode sulfurization only, which occurs via electrochemical mechanisms mainly [16-19]. At low hydrogen sulfide levels just two poisoning reaction types occur: physical and chemical absorptions on nickel surface; replacement of carbonate ions with sulfide and sulfate ions. In fact, formations of bulk nickel sulfides are thermodynamically forbidden. However, when an electrical load is applied at the cell, the anodic potential increases up to right values for nickel sulfide formations via electrochemical mechanisms. It means that when MCFC works, the cell component materials are more sensible to hydrogen sulfide attack. When the cell is fed with clean anodic gas, it recovers the original performance because the poisoning reaction is reversible. However, the performance recovering is not total. the irreversible poisoning effects are due to stable nickel sulfide formations, $\mathrm{Ni_3S_2}$. The aim of this work is focused on developing sulfur resistant anode materials for MCFC fed with biogas in order to improve the fuel cell reliability without compromising the performance.

The innovative material, which is nanostructured NiCr (5%) alloy covered with a thin layer of CeO_2, was prepared, characterized and tested in fuel cell. The ceria coating acts as sacrificial material for sulfur entrapping by the reaction

$$2CeO_2 + H_2S + H_2 \rightarrow Ce_2O_2S + 2H_2O. \tag{5}$$

2. – Experimental work

2˙1. *Synthesis of anode materials.* – A conventional porous anode made of nanostructured nickel was prepared by tape casting method. The casted slurry, containing nickel and chromium powder, the polymeric binder, the organic solvent, the dispersant and the plasticizer, forms a tape whose thickness is controlled by a doctor blade. The green tape was dried at room temperature and sintered at 1173 K under a reducing atmosphere. After that, the sintered tape was pre-oxidized in order to form thin layer of chromium oxide at the nickel grain boundaries, interfering with surface diffusion of nickel atoms and prevent a recrystallization and sintering of porous nickel while it works as electrode. The innovative anode was made covering the conventional anode with a thin layer of ceria by dip-coating from sol-gel. The sol was prepared with $(NH_4)_2Ce(NO_3)_6$ and NH_3. The gel transition was started by adding ascorbic acid as complexing agent. The pre-oxidized conventional anode is suitable for dip-coating because the chromium oxide restrains the sol-gel and promote the homogeneous coating of the surface. After dip-coating, the sample was dried at 100 °C and calcined at 600 °C in order to have a thin layer of ceria on nickel surface.

2˙2. *Anode materials characterization.* – The morphology characterization was performed by means of the Scanning Electron Microscope (SEM) and the Energy-Dispersive X-ray (EDX) analyses by using the JEOL JSM-5510LV instrument. The phase identifications and crystalline structure were performed by X-Ray Diffraction (XRD) by using a Rigaku Miniflex diffractometer with Cu-K_α radiation (tube output voltage 30 kV and tube output current 15 mA) and scanning range from $2\theta = 3°$ to $2\theta = 90°$ (step 0.02° and rate 2°/min). Raw data were submitted to three processes: smoothing process by Savitzky method; background elimination process by Sonnevelt method; $K_\alpha 2$ elimination process.

2˙3. *Fuel cell testing.* – In order to compare the performance of the innovative anode materials with the conventional one, two differ cells was assembled, having the same cathode and tile but different anodes: the cathode material was a porous lithiated nickel oxide; the tile was made of a porous lithium aluminate matrix containing a binary solution of carbonate salts at the eutectic composition, Li_2CO_3:K_2CO_3 = 62:38 mol%; the anode materials was NiCr (5%) for one cell and NiCr (5%) covered with ceria for the other one. A 100 cm^2 class MCFC was used in this work in order to investigate the sulfur poisoning effects in bench-scale single-cell testing. The geometric surface area of each electrode was 55 cm^2; but the actual electroactive area is larger than geometric one because of the electrode porosity. Experimental conditions were as follows: temperature 650 °C; pressure 1 atm; composition of the cathode inlet gas O_2:N_2:CO_2 = 14.4:54.2:31.4 vol%, composition of the anode inlet gas H_2:H_2O:CO_2:N_2 = 25:25:4:46 vol%. Different amount of hydrogen sulfide, such as 2 ppm, 4 ppm and 6 ppm, was introduced successively in the anode side. Cell performances were tested by means of the AgilentN333 instrument. Galvanostatic analyses were performed by applying various constant direct currents and

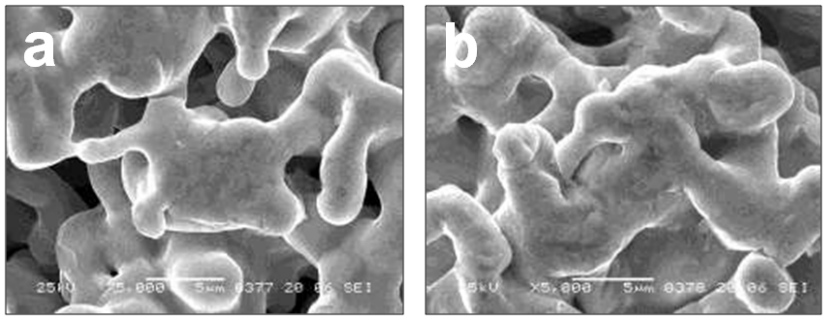

Fig. 3. – SEM images of the conventional anode: a) before preoxidation; b) after preoxidation.

recording the cell voltages at steady-state conditions. From these measures it was possible to draw the polarization curves by graphing potential cells at steady state condition against the current density. A custom-compiled LabView program was used to control the test rig and data acquisition.

3. – Results and discussion

Figure 3 shows the conventional anode before and after the pre-oxidation step. It is evident that the anode keeps the nanostructure even if chromium oxides form thin layers on the nickel grain boundaries. After dip-coating, the anode surface is homogeneously covered with the sol-gel of ceria precursors, fig. 4a. After calcination at 600 °C, the layer thickness of the formed ceria is thin enough to not alter or destroy the nanostructures and porosity of the anode, fig. 4b. EDX analysis is an useful method for mapping the cerium element, fig. 5, and confirming that the ceria oxide distribution is homogeneous both on surface and into the pores along the cross section of the anode.

As already mentioned, two kinds of fuel cells are assembled: one cell has a conventional anode and the other cell has the innovative anode. Both fuel cells are subjected to consecutive three steps for each poisoning level: in the initial step, the cells are fed with clean anode gas (H_2:H_2O:CO_2:N_2 = 25:25:4:46%); in the poisoning step, the cells are fed

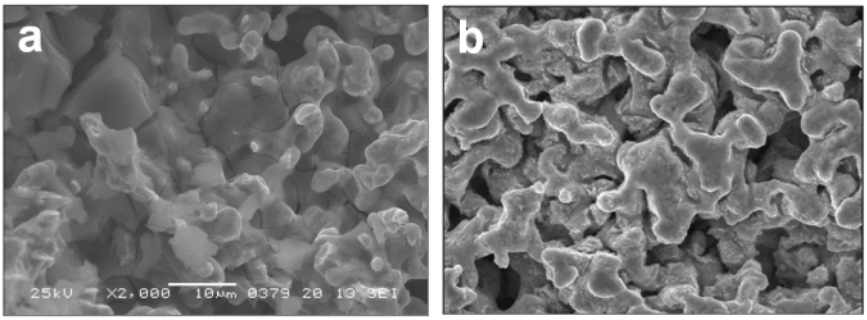

Fig. 4. – SEM images of the innovative anode: a) before calcinations at 600 °C; b) after calcinations at 600 °C.

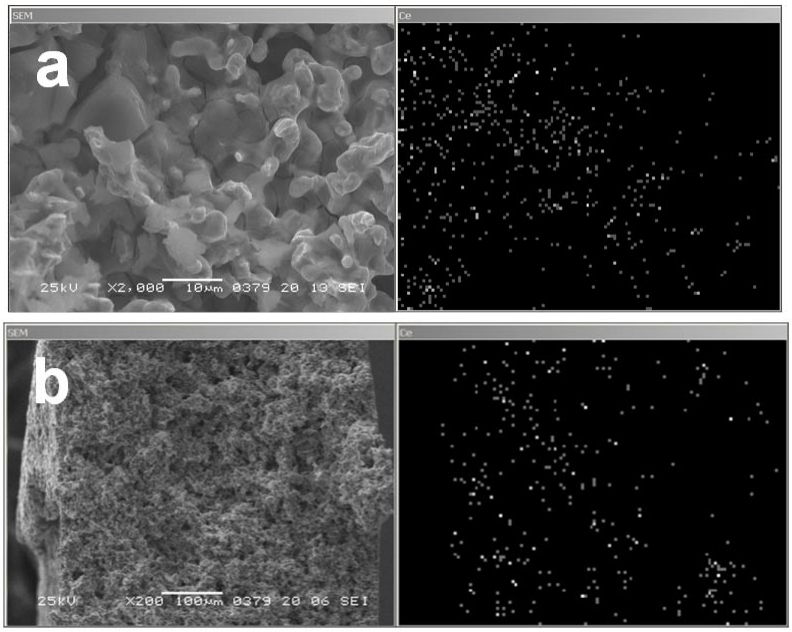

Fig. 5. – SEM images and EDX elemental mapping of Cerium: a) surface; b) cross-section.

with dirty anode gas (H_2:H_2O:CO_2:N_2 = 25:25:4:46% and 2, 4 and 6 ppm of H_2S); in the recovering step, the cells are fed with clean anode gas (H_2:H_2O:CO_2:N_2 = 25:25:4:46%). Comparing the polarization curves, it is evident that the sulfur poisoning effects on cell performances are reduced by using innovative anode. Indeed, the sulfur poisoning start to be significant at higher hydrogen sulfide level, 6 ppm instead of 4 ppm. In addition, considering the poisoning at 6 ppm, the performance recovering is almost full when the anode is made of nickel chromium alloy covered with a thin layer of ceria oxide, fig. 6.

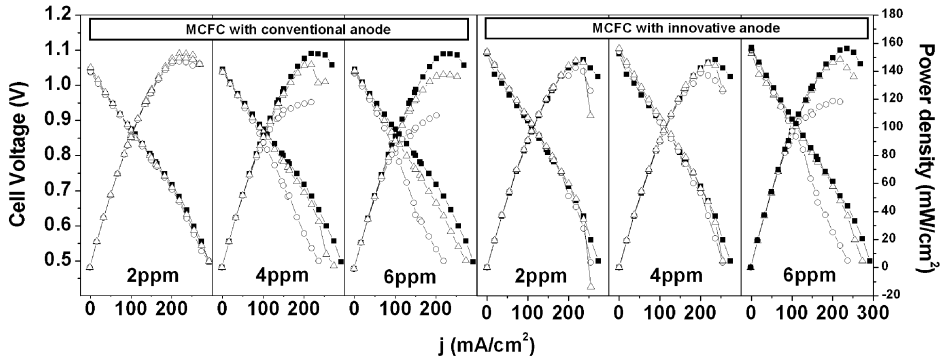

Fig. 6. – Polarization curves for MCFC with conventional anode and with innovative anode over the initial step (black square), the poisoning step (white circle) and the recovering step (white triangle).

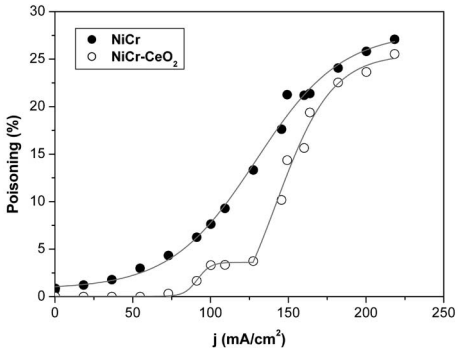

Fig. 7. – Cell voltage drop percentage due to sulfur poisoning as function of current density, related to 6 ppm of hydrogen sulfide.

Figure 7 shows the cell voltage drop percentage due to the poisoning at 6 ppm hydrogen sulfide as a function of current density. The curve related to the poisoning against the innovative anode has a two-stairs-shape, showing that the poisoning includes two steps. The first step occurs at low current density, from 0 mA/cm^2 up to 150 mA/cm^2, where only the covering layer is sulfured because of chemical poisoning reactions against ceria. The curve reach the first plateau, when ceria becomes saturated with sulfur and the system is under a dynamic steady state condition without significant poisoning effects. The second step begins at 150 mA/cm^2, when the free ceria for sulfur entrapping is over and the anode potential has the right value for promoting the electrochemical poisoning reactions against nickel. The curve reach the second plateau, when nickel becomes saturated with sulfur and the system is under a new dynamic steady state condition.

The claimed two-step pathway for sulfur poisoning against the coated anode is in agreement with fig. 8, where the recovering percentages are showed. Referring to the coated anode, when the only coating layer is sulfured, occurring at low current density, the recovering is completely full because of the redox properties of ceria. On the other hand, when both the ceria coating layer and the nickel support are sulfured, occurring at high current density, the recovering is not more full because of the formation of Ni_3S_2,

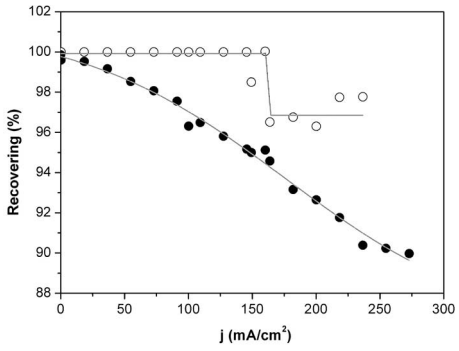

Fig. 8. – Recovering percentage as function of current density, related to 6 ppm of hydrogen sulfide.

the thermodynamically stable nickel sulfide. Even if the recovering is partial, it is almost complete, 98%, rather than that of the anode without ceria coating, 90%. Indeed the ceria layer can promote the nickel desulfuration by the reaction

$$\text{NiS} + 2\text{CeO}_2 + 2\text{H}_2 \rightarrow \text{Ni} + \text{Ce}_2\text{O}_2\text{S} + 2\text{H}_2\text{O}. \tag{6}$$

4. – Conclusion

A multidisciplinary research in energy technology address global warming, air pollution, global energy security and local energy independence issues. In particular, bioenergy produced by fuel cell devices plays a key role as solution for energy, environmental and socio-economic sustainability. Molten carbonate fuel cell is particularly suitable for bioenergy production because it can be fed directly with biogas, whose primary constituents all improve the performance of the cell. However hydrogen sulfide, which is the main biogas impurity, poisons the conventional nickel based anode, affecting the power and the endurance of the cell. In order to overcome this problem, it has been developing innovative anode materials that resist against the sulfide corrosions. The performances of the conventional anode are compared with those of the innovative one, made of nickel-chromium alloy covered with ceria. Two MCFCs, having the same cathode and tile but different anode, are tested by monitoring the performance and doing post-service analyses. Experimental result confirms that the nanostructured and porous innovative anode gives more stable performance than that of the conventional one because ceria traps hydrogen sulfide, acting as a sacrificial material. The sulfur poisoning against the innovative anode can be described by a two-step pathway. The first step includes the chemical sulfuration of ceria because Ce^{+4} is quickly reduced to Ce^{+3} forming Ce_2O_2S in agreement with the redox properties of ceria. The second step includes the electrochemical sulfuration of nickel because at high current density the electrochemical poisoning reaction is favored. For that reason, when MCFC is continuously fed with biogas, ceria coating layer removes short-term spikes in relatively high hydrogen sulfide concentration, preventing the anode degradation. After the hydrogen sulfide spike, ceria recovers the original trapping ability because sulfur is almost completely desorbed when the clean anodic gas feed the cell. Finally, the studied innovative materials are suitable for producing advanced anode for fuel cell fed with biogas, the core of an integrated power plant promoting renewable source and high energy conversion efficiency.

* * *

The authors acknowledge financial support from the Italian Ministry of Economic Development (Project 09A05805, CERSE 2009-2011).

REFERENCES

[1] Deptuła A., Miłkowska M., Łada W., Olczak T., Wawszczak D., Smolinski T., Brykala M., Chmielewski A. G., Zaza F. and Goretta K. C., *Adv. Mater. Res.*, **518-523** (2012) 3216.
[2] Mckendry P., *Bioresour. Technol.*, **83** (2002) 37.
[3] Mckendry P., *Bioresour. Technol.*, **83** (2002) 47.
[4] Pozio A., Zaza F., Masci A. and Silva R. F., *J. Power Sources*, **179** (2008) 631.
[5] Paoletti C., Carewska M., Lopresti R., Mcphail S., Simonetti E. and Zaza F., *J. Power Sources*, **193** (2009) 292.

[6] Paoletti C., Zaza F., Carewska M., Lopresti R. and Simonetti E., *J. Fuel Cell Sci. Techol.*, **7** (2010) 021008.
[7] Pozio A., Cemmi A., Carewska M., Paoletti C. and Zaza F., *J. Fuel Cell Sci. Technol.*, **7** (2010) 041003.
[8] Frangini S., Masci A. and Zaza F., *Corros. Sci.*, **53** (2011) 2539.
[9] Frangini S., Zaza F. and Masci A., *Corros. Sci.*, **62** (2012) 136.
[10] Ciccoli R., Cigolotti V., Lopresti R., Massi E., Mcphail S. J., Monteleone G., Moreno A., Naticchioni V., Paoletti C., Simonetti E. and Zaza F., *Waste Manage*, **30** (2010) 1018.
[11] Sasaki K., *J. Fuel Cell Sci. Technol.*, **5** (2008) 031212.
[12] Watanabe T., Izaki Y., Mugikura Y., Morita H., Yoshikawa M., Kawase M., Yoshiba F. and Asano K., *J. Power Sources*, **160** (2006) 868.
[13] Sammells A. F., Nicholson S. B. and Ang P. G. P., *J. Electrochem. Soc.*, **127** (1980) 350.
[14] Kawase M., Mugikura Y. and Watanabe T., *J. Electrochem. Soc.*, **147** (2000) 1240.
[15] Uchida, Ohuchi S. and Nishina T., *J. Electroanal. Chem.*, **369** (1994) 161.
[16] Zaza F., Paoletti C., Lopresti R., Simonetti E. and Pasquali M., *18th European Biomass Conference and Exhibition* (ETA-Florence Renewable Energie) (2010) ISBN 978-88-89407, 1816.
[17] Zaza F., Paoletti C., Lopresti R., Simonetti E. and Pasquali M., *J. Power Sources*, **195** (2010) 4043.
[18] Zaza F., Paoletti C., Lopresti R., Simonetti E. and Pasquali M., *Int. J. Hydrogen Energ.*, **36** (2011) 8119.
[19] Devianto H., Simonetti E., Mcphail S. J., Zaza F., Cigolotti V., Paoletti C., Moreno A., La Barbera A. and Luisetto I., *Int. J. Hydrogen Energ.*, **37** (2012) 19312.